Northumbria Research Link

www.northumbria.ac.uk/nrl

northumbria
UNIVERSITY NEWCASTLE

Multi-User Visible Light Communication Broadcast Channels With Zero-Forcing Precoding

Thanh V. Pham, *Student Member, IEEE*, Hoa Le-Minh, *Member, IEEE*, and Anh T. Pham, *Senior Member, IEEE*

Abstract—This paper studies zero-forcing (ZF) precoding designs for multi-user multiple-input single-output visible light communication (VLC) broadcast channels. In such broadcast systems, the main challenging issue arises from the presence of multi-user interference (MUI) among non-coordinated users. In order to completely suppress the MUI, ZF precoding, which is originally designed for radio frequency (RF) communications, is adopted. Different from RF counterpart, VLC signal is inherently non-negative and has a limited linear range, which leads to an amplitude constraint on the input data signal. Unlike the average power constraint, obtaining the exact capacity for an amplitude-constrained channel is more cumbersome. In this paper, we first investigate lower and upper bounds on the capacity of an amplitude-constrained Gaussian channel, which are especially tight in the high signal-to-noise regime. Based on the derived bounds, optimal beamformer designs for the max–min fairness sum-rate and the maximum sum-rate problems are formulated as convex optimization problems, which then can be efficiently solved by using standard optimization packages.

Index Terms—VLC, multi-user MISO, precoding, max-min fairness, sum-rate maximization.

I. INTRODUCTION

THE ever-increasing demand for high data-rate wireless communications has spurred a rapid progress in the research and development of visible light communication (VLC) technology. Exploiting the massive deployment of light emitting diodes (LEDs), VLC is expected to serve as a possible complement to the existing wireless technologies in the future indoor networking. This is mainly due to a number of advantages brought by VLC: dual functionalities (illumination and communications), license-free spectrum, high signal-to-noise ratio (SNR) and high security to name a few [1]–[4]. To open the road for commercialization, VLC has also been standardized for wireless personal area networks (WPANs) in IEEE 802.15.7 [5].

Despite the promising benefits, practical deployment of VLC systems faces numerous challenges in which achieving

high data rate is one of the major concerns due to the limited modulation bandwidth of the LED. Extensive research effort has been devoted to the data rate improvement of VLC systems [6]–[9]. Among proposed methods, multiple-input multiple-output (MIMO) is one of potential solutions by exploiting the spatial multiplexing gain. Some experiments have demonstrated that high data rates up to gigabits/s can be achieved with the combination of MIMO and orthogonal frequency division multiplexing (OFDM) technologies. The use of multiple separated LED sources to form the MIMO transmission is also natural since it helps to guarantee the illumination standard (typically > 300 lux) for lighting a large room/office.

A number of studies on MIMO-VLC systems, including both theoretical analysis and experimental demonstrations, have been recently reported [9]–[15]. In these studies, VLC systems with one receiver (unicast transmission) were examined. VLC networks can be nevertheless categorized as broadcast networks, which are able to serve multiple users simultaneously, due to the broadcast nature of visible light signal. This is regarded as multi-user (MU) MIMO-VLC broadcast systems which are analogous to the RF ones; and the presence of multiple users, which results in the so-called MU interference (MUI), consequently degrades the performance.

It is generally difficult to handle the MUI at receivers when there is no coordination among them. As a result, MUI effect mitigation should be done at the transmitter side. This is the idea behind precoding techniques applied in MU broadcast channel by pre-processing the transmit signal before transmission. Precoding techniques for RF broadcast channels have been extensively investigated [16]–[19]. Nevertheless, adoption of those techniques for VLC is not straightforward because the RF signal is complex-valued, which is fundamentally different from the real and non-negative VLC signal.

Several studies on precoding design for MU-VLC systems, which mainly focus on linear precoding algorithms with either mean square error (MSE) or zero-forcing (ZF) criterion, have been reported. In particular, for the case of multiple photodiodes (PDs) at the receivers, i.e. MU-MIMO configuration, [20]–[22] studied the use of block diagonalization (BD) precoding [17] which can be regarded as a generalization of the ZF precoding. It is noted that our study in [22] is the first work that took into account the non-negativity signal constraint in designing the BD precoding for MU-MIMO VLC systems. In case of single-PD receivers, or the MU-MISO configuration, precoding matrices based on the MSE criterion were designed to minimize the sum MSE [23] or to minimize the maximum MSE among users, i.e., max-min fairness MSE, [24].

Following these studies, the sum-rate performance of MU-MISO VLC systems with ZF precoding, one of the most critical performance metrics in multiuser systems, is reported [25], [26]. There are nevertheless two important limitations in these studies. ***Firstly,*** these studies in fact did not consider the sum-rate in terms of *channel capacity*, which is defined as the maximum mutual information between the input and the output for which an arbitrarily small bit error-rate (BER) can be achieved. On the contrary, the sum-rate optimization problem is formulated by adopting the expression in [29, eq. (24)], which particularly specifies the *achievable data rate* for an optical intensity modulation/direct detection (IM/DD) channel with multi-level *M*-ary pulse amplitude modulation (PAM) given a minimum BER threshold. By doing so, the problems could be formed as convex optimization ones (which then can be solved by standard optimization packages) because the achievable data rate expression depends on the ratio of the amplitude signal to the standard deviation of noise, i.e., root square of the SNR in [25] and [26].

Secondly, it is well-known that ZF precoding design has a close relationship with the concept of generalized inverse in linear algebra as its function is to invert the MU channel. In previous studies, the ZF precoding was chosen in the form of pseudo-inverse, a special generalized inverse of the channel matrix, which has been proved to achieve the optimal precoding design in MU-RF systems with average power constraint [16]. In VLC systems nevertheless, the combination of peak power due to the limited linear range (further elaboration in the next Section) and non-negativity signal results in amplitude constraint. The pseudo-inverse therefore may not necessarily result in the optimal solution.

This paper attempts to tackle both limitations. First, we examine the sum-rate performance of MU-MISO VLC systems in terms of the *channel capacity* with the amplitude constraint. It is necessary to note that the study on lower bound on the VLC channel capacity of MU-MISO VLC systems with the amplitude constraint was reported in [27] and [28]. In this paper, we extend these studies by the derivation of an upper bound and other two lower bounds with different degrees of tightness. Asymptotic behaviors of these bounds will be also discussed to confirm their validity in characterizing the sum-rate performance. Secondly, we solve the sum-rate optimization problems according to the considered bounds, and prove that the pseudo-inverse is not necessarily the optimal solution under the amplitude constraint. Finally, two iterative algorithms are proposed to find the generalized inverse solutions for the optimal precoding designs in the case of sum-rate maximization. Convergence behaviors of the proposed algorithms will also be evaluated to validate their efficiency.

It is important to highlight that the capacity-achieving distribution for the amplitude-constrained Gaussian scalar channel is discrete with a finite number of mass points, and from this observation, a numerical algorithm was developed to determine the capacity and the optimal input distribution [30]. In addition to the exact solution, several closed-form lower and upper bounds were also derived in [31], [32], and [35]. Furthermore, in the case of broadcast systems with precoding,

both precoding matrices and the input distribution should be, in principle, jointly optimized to compute the channel capacity. To the best of our knowledge, there has been no study on this problem. In this paper, instead of finding an exact solution, we investigate a suboptimal approach by omitting the optimal input distribution condition. In particular, we rely on previously proposed capacity bounds for scalar Gaussian channels and focus on the optimal ZF precoding design.

The remainder of the paper is organized as follows. In Section II, we revisit the issue of scalar Gaussian channel capacity with an amplitude signal constraint. Simple lower and upper bounds of the capacity are provided as benchmarks for the precoding designs in the MU scenario. Section III introduces the model of MU-MISO VLC broadcast systems, linear precoding scheme and the discussion on amplitude constraint on LEDs. A brief review of ZF precoding is provided in Section IV. In Section V, we present the optimal precoding matrix designs with respect to lower and upper capacity bounds for the max-min fairness and the maximum sum-rate criterions, respectively. Numerical results and discussions are given in Section VI, and finally, we conclude the paper in Section VII.

Notation: The following notations are used throughout the paper. Bold upper case letters represent matrices, e.g., $\mathbf{A}$. The transpose of matrix $\mathbf{A}$ is written as $\mathbf{A}^T$, while $[\mathbf{A}]_{i,j}$ indicates the element at the i−th row and the j−th column and $[\mathbf{A}]_{k,:}$ denotes the k−th row vector of $\mathbf{A}$. $\|\cdot\|_F$ and $\|\cdot\|_1$ are the Frobenius norm and the L_1 norm operators, respectively. $\mathbb{R}$, $\mathbb{R}^+$ are the real and positive real number sets. $\mathbb{I}(\cdot;\cdot)$ and $h(\cdot)$ represent the mutual information and the differential entropy in *nats*, respectively. Expected value is denoted by $\mathbb{E}[\cdot]$ and the natural logarithm $\log(\cdot)$ is used. Finally, sup denotes the supremum operator and $|\cdot|$ is the absolute value operator.

II. INFORMATION CAPACITY OF AMPLITUDE-CONSTRAINED SCALAR GAUSSIAN CHANNELS

In this section, we revisit the capacity of scalar Gaussian channels with an amplitude input signal constraint. Simple closed-form expressions for the lower and upper bounds capacity are provided as benchmarks for the capacity analysis in the multiuser scenario. Smith [30], considered a scalar additive Gaussian noise channel characterized by

$$Y = X + N, \qquad (1)$$

where X, N, and Y denote the channel input, noise, and output random variables, respectively. The input random variable X is assumed to be constrained to take on values on $[-A, A]$ for some arbitrary positive value of A.[1] The noise random variable N is assumed to be Gaussian with zero mean and variance N_0. The capacity-achieving distribution of X for the channel in (1) is unique and discrete with a finite number of mass points. Necessary and sufficient conditions for the distribution were obtained and the capacity was computed numerically.

---

[1]The channel in (1) is sometimes referred as the Gaussian channel with peak power constraint since the amplitude constraint $X < |A|$ is equivalent to the peak power constraint $X^2 < A^2$.

Nevertheless, it is worth noting that the developed numerical procedure was quite computationally expensive especially for large value of $\frac{A}{N_0}$. Therefore, closed-form expressions for the capacity are of particular interest for system design purpose.

A. Lower Bound

For additive noise channels, one common way to derive a lower bound capacity is to use the Entropy Power Inequality (EPI) [31], [33] as

$$
\begin{aligned}
C_L^1 &= \mathbb{I}(X;Y) = h(Y) - h(Y|X) \\
&= h(X+N) - h(N) \\
&\overset{(\text{EPI})}{\geq} \frac{1}{2}\log\left(e^{2h(X)} + e^{2h(N)}\right) - h(N) \\
&= \frac{1}{2}\log\left(1 + \frac{e^{2h(X)}}{2\pi e N_0}\right).
\end{aligned}
\tag{2}
$$

To make this bound as tight as possible, the distribution of X is chosen in such a way that maximizes the differential entropy $h(X)$ under the amplitude constraint $X \leq |A|$. According to the maximum entropy theorem [34], it is well-known that the uniform distribution is the maximum entropy probability distribution for a random variable under no constraint other than it is contained in the distribution's support. It is thus reasonable to assume that X is uniformly distributed over $[-A, A]$, resulting in

$$
C_L^1 = \frac{1}{2}\log\left(1 + \frac{2A^2}{\pi e N_0}\right).
\tag{3}
$$

From the above expression, it is straightforward to derive another bound as

$$
\begin{aligned}
C_L^2 &\geq \frac{1}{2}\log\left(1 + \frac{2A^2}{\pi e N_0}\right) > \frac{1}{2}\log\left(\frac{2A^2}{\pi e N_0}\right) \\
&= \log\left(\frac{2A}{\sqrt{2\pi e N_0}}\right).
\end{aligned}
\tag{4}
$$

B. Upper Bound

An upper bound for the capacity of a scalar Gaussian channel with an amplitude constraint is given by [35]

$$
C_U = \sup_{\alpha \in [0,1]} f(\alpha),
\tag{5}
$$

where $f(\alpha) = \alpha \log\left(\frac{2A}{\sqrt{2\pi e N_0}}\right) - \log\left(\alpha^\alpha (1-\alpha)^{\frac{3}{2}(1-\alpha)}\right)$. It is seen that $f(\alpha)$ is twice differentiable and is a concave function on its domain $\alpha \in [0, 1]$ due to the concavity of the logarithm function. Therefore, the maxima of $f(\alpha)$ can be found by finding the critical point α^*, (the point where $f'(\alpha^*) = 0$). In appendix , we show that α^* exists and is unique. Moreover, α^* can be numerically found by using the bisection method, i.e., narrowing down the interval of α by halves over iteration by iteration [36]. With a predefined error tolerance $\nu = 10^{-3}$ and an initial interval of $[0, 1]$, α^* can be obtained after around 15 iterations.
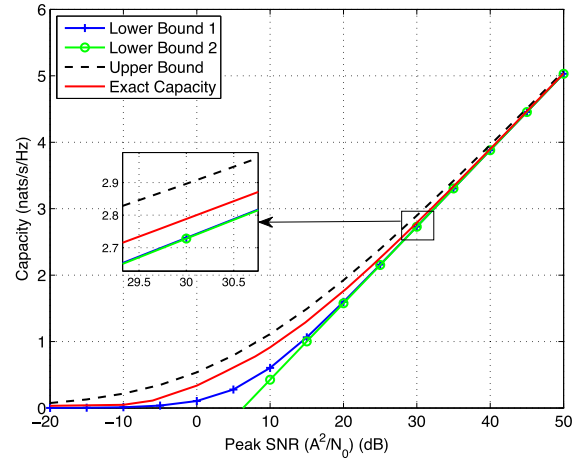
Fig. 1. Exact, lower and upper bounds capacities of amplitude-constrained scalar Gaussian channels.
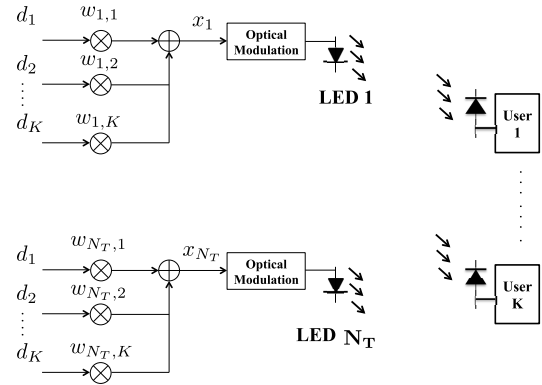
Fig. 2. Schematic diagram of a MU-MISO VLC system.

C. Asymptotic Behaviors

Figure 1 shows the exact, the lower and the upper bounds capacity versus the peak SNR of an amplitude-constrained Gaussian channel. It is seen that the upper bound and the lower bound in (3) are tight at low and hight peak SNR regimes, whereas the lower bound in (4) is tight at high SNR region only. Obviously, for two lower bounds, $\lim_{\frac{A}{\sqrt{N_0}} \to 0} C_L^1 = 0$ and $\lim_{\frac{A}{\sqrt{N_0}} \to 0} C_L^2 = -\infty$. The following proposition proves the tightness of the upper bound at low and high peak SNR regimes.

Proposition 1: Asymptotic behaviors of the upper bound

$$
\lim_{\frac{A}{\sqrt{N_0}} \to 0} C_U = 0,
\tag{6}
$$

$$
\lim_{\frac{A}{\sqrt{N_0}} \to \infty} C_U = \log\left(\frac{2A}{\sqrt{2\pi e N_0}}\right).
\tag{7}
$$

Proof: See Appendix .

III. MU-MISO VLC SYSTEM MODEL

A. MU-MISO VLC Channel Model

Figure 2 illustrates the schematic diagram of a MU-MISO VLC system with N_T LED arrays as transmitters and

K decentralized single-photodiode users. For indoor VLC systems, there are generally two main types of link model, which are the direct light-of-sight (LOS) and the non-direct line-of-sight (NLOS). In most cases, only LOS link is taken into account since it accounts for more than 95% of the total received optical power at the receiver [38]. Quantitatively, even the strongest NLOS path component is at least 7 dB lower than the weakest LOS one [9]. For the sake of simplicity, we thus consider the LOS propagation path in this study. Let $\mathbf{H}_k \in \mathbb{R}^{1 \times N_T}$ be the channel matrix between LED arrays and the $k-$th user

$$\mathbf{H}_k = \begin{bmatrix} h_{k1} & h_{k2} & \cdots & h_{kN_T} \end{bmatrix}, \tag{8}$$

where h_{ki} represents the direct current (DC) gain between the $k-$th user and the $i-$th LED array. In practice, most LED sources have Lambertian beam distribution where the emission intensity is given as

$$L(\phi) = \frac{l+1}{2\pi} \cos^l(\phi), \tag{9}$$

with ϕ is the angle of irradiance and l is the order of Lambertian emission determined by the semi-angle for half illuminance of the LED $\Phi_{1/2}$ as $l = \frac{-\log(2)}{\log(\cos \Phi_{1/2})}$. For LOS link, h_{ki} is given by [38]

$$h_{ki} = \begin{cases} \frac{A_r}{d_{ki}^2} L(\phi) T_s(\psi_{ki}) g(\psi_{ki}) \cos(\psi_{ki}), & 0 \le \psi_{ki} \le \Psi_c, \\ 0, & \psi_{ki} > \Psi_c, \end{cases} \tag{10}$$

where A_r and d_{ki} are the active area of the PD and the distance from the LED array to the PD, respectively. ψ_{ki} is the angle of incidence, $T_s(\psi_{ki})$ is the gain of the optical filter and Ψ_c denotes the optical field of view (FOV) of the PD. $g(\psi_{ki})$ is the gain of the optical concentrator and given by

$$g(\psi_{ki}) = \begin{cases} \frac{\kappa^2}{\sin^2 \Psi_c}, & 0 \le \psi_{ki} \le \Psi_c, \\ 0, & \psi_{ki} > \Psi_c, \end{cases} \tag{11}$$

where κ is the refractive index of the concentrator.

B. Precoding Model and Broadcast Transmission

In the considered MU-MISO VLC system, N_T LED arrays cooperate to broadcast information to K users simultaneously. This configuration can be regarded as a *coordinated multi-point* (CoMP) system for VLC communications [23]. In our study, a DC-biased PAM scheme is employed. In such scheme, a DC bias current $I_{DC} \in \mathbb{R}^+$ which determines the brightness of the LEDs, is used to modulate a zero-mean data signal. Let $d_i \in \mathbb{R}$ be the data symbol intended for the i-th user, and $\mathbf{d} = \begin{bmatrix} d_1 & d_2 & \dots & d_K \end{bmatrix}^T \in \mathbb{R}^{K \times 1}$ be the data vector for all users. It is assumed that d_i is zero-mean, and without loss of generality, is normalized to the range of $[-1, 1]$ [14]. At the $k-$th LED array, the broadcast signal s_k which consists of data signals for all users, is generated from a linear combination of the data vector and the matrix $\mathbf{V}_k = \begin{bmatrix} w_{k,1} & w_{k,2} & \dots & w_{k,K} \end{bmatrix} \in \mathbb{R}^{1 \times K}$ as

$$s_k = \mathbf{V}_k \mathbf{d}, \tag{12}$$

As a result, the transmitted signal x_k can be expressed in the form of

$$x_k = s_k + I_{DC}^k, \tag{13}$$

where I_{DC}^k denotes the DC-bias for the $k-$ LED array [15]. Since $\mathbf{E}[d_k] = 0$, the signal s_k does not affect the average illumination level of the LEDs. Instead, it is uniquely determined by the DC-bias I_{DC}^k. If we define $\mathbf{x} = \begin{bmatrix} x_1 & x_2 & \dots & x_K \end{bmatrix}^T \in \mathbb{R}^{K \times 1}$ as the transmitted signal vector and $\mathbf{I}_{DC} = \begin{bmatrix} I_{DC}^1 & I_{DC}^2 & \dots & I_{DC}^K \end{bmatrix}^T \in \mathbb{R}^{K \times 1}$ as the aggregate DC bias vector, the received optical signal at the $k-$th user can be written as

$$P_r^k = \mathbf{H}_k \mathbf{P}_s, \tag{14}$$

where $\mathbf{P}_s = \begin{bmatrix} P_s^1 & P_s^2 & \dots & P_s^{N_T} \end{bmatrix}^T \in \mathbb{R}^{N_T \times 1}$ is the transmitted optical power vector of the LED arrays whose element $P_s^k = \eta x_k$ is the transmitted optical power of the $k-$th LED arrays with η is the LED conversion factor. The received electrical signal at the $k-$th user after the optical-electrical conversion is therefore given by

$$\begin{aligned} y_k &= \gamma P_r^k + n_k = \gamma \eta \mathbf{H}_k \mathbf{x} + n_k \\ &= \gamma \eta \left(\mathbf{H}_k \mathbf{W}_k d_k + \mathbf{H}_k \sum_{i=1, i \ne k}^{K} \mathbf{W}_i d_i + \mathbf{H}_k \mathbf{I}_{DC} \right) + n_k, \end{aligned} \tag{15}$$

with γ is the PD responsivity, $\mathbf{W}_k = \begin{bmatrix} w_{1,k} & w_{2,k} & \dots & w_{N_T,k} \end{bmatrix}^T \in \mathbb{R}^{N_T \times 1}$ is the *precoder* for the $k-$th user. If we define $\mathbf{W} = \begin{bmatrix} \mathbf{W}_1 & \mathbf{W}_2 & \dots & \mathbf{W}_K \end{bmatrix} \in \mathbb{R}^{N_T \times K}$, it can be seen that $\mathbf{W}$ can also be represented as $\mathbf{W} = \begin{bmatrix} \mathbf{V}_1 & \mathbf{V}_2 & \dots & \mathbf{V}_{N_T} \end{bmatrix}^T$, where the $k-$th row vector is the *precoder* for the $k-$th LED array.

As seen in (15), the first term $\mathbf{H}_k \mathbf{W}_k d_k$ is the desired signal, while the second term $\mathbf{H}_k \sum_{i=1, i \ne k}^{K} \mathbf{W}_i d_i$ is the MUI. The third term $\mathbf{H}_k \mathbf{I}_{DC}$ represents the DC current for defining the illumination that carries no data and n_k denotes the receiver noise, which is assumed to be additive white Gaussian noise (AWGN) with zero mean and variance σ_k^2, given by

$$\sigma_k^2 = 2e \overline{P_r^k} B + 4\pi e A_r \gamma \chi_{\text{amb}} (1 - \cos(\Psi_c)) B + i_{\text{amb}}^2 B, \tag{16}$$

where e is the elementary charge, B denotes the system bandwidth and $\overline{P_r^k} = \mathbb{E}[P_r^k] = \eta \mathbf{H}_k \mathbf{I}_{DC}$ is the average received optical power at the $k-$th user. i_{amp}^2 is the pre-amplifier noise current density, χ_{amp} is the ambient light photocurrent. After removing the DC current by AC coupling, the received signal can be written by

$$y_k = \gamma \eta \left(\mathbf{H}_k \mathbf{W}_k d_k + \mathbf{H}_k \sum_{i=1, i \ne k}^{K} \mathbf{W}_i d_i \right) + n_k. \tag{17}$$

C. Amplitude Constraint on VLC Signal

In this section, we briefly illustrate signal amplitude constraint in VLC systems, which is fundamentally different from their RF counterpart. It should be noted that the constraint,
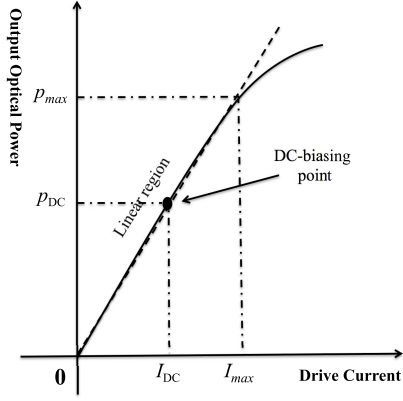
Fig. 3. Nonlinear LED transfer characteristic.

in turn, affects significantly the design of precoding matrices. As shown in Fig. 3, the LEDs exhibit a limited linear range, where the output optical power increases linearly from 0 to $p_{\max}$ in accordance with the input drive current from 0 to $I_{\max}$. Hence, to guarantee normal operation of the LEDs, i.e., to avoid the overheating of the LEDs and the potential light intensity reduction, the drive current x_k for the $k-$th LED array must be constrained within the range of $[0, I_{\max}]$ as

$$0 \le s_k + I_{\mathrm{DC}}^k \le I_{\max}. \qquad (18)$$

From (12) and since $|d_k| \le 1$, we get

$$-\left\|\mathbf{V}_k\right\|_1 \le s_k \le \left\|\mathbf{V}_k\right\|_1. \qquad (19)$$

To ensure both (18) and (19), the following constraint should be imposed

$$\left\|\mathbf{V}_k\right\|_1 \le \Delta_k, \qquad (20)$$

where $\Delta_k = \min\left(I_{\mathrm{DC}}^k, I_{\max} - I_{\mathrm{DC}}^k\right)$. We can write the above constraint with respect to $\mathbf{W}_i$ or $\mathbf{W}$ as

$$\sum_{i=1}^{K} \left\|[\mathbf{W}_i]_{k,:}\right\|_1 \le \Delta_k, \qquad (21)$$

or

$$\left\|[\mathbf{W}]_{k,:}\right\|_1 \le \Delta_k. \qquad (22)$$

In this paper, depending on the targeted performance metric, either the expression in (21) or (22) will be considered in the design of the optimal precoding matrices.

IV. ZF PRECODING

The goal of the transmit precoding is to mitigate the negative impact of the MUI term in the received signal (see (17)). In particular, the ZF precoding algorithm aims to completely remove the MUI via the construction of the precoder $\mathbf{W}_i$ in such a way that it is orthogonal to channel matrices of other users, i.e.,

$$\mathbf{H}_k \mathbf{W}_i = 0, \quad \forall k \ne i. \qquad (23)$$

In other words, if we define $\mathbf{H} = \begin{bmatrix} \mathbf{H}_1^T & \mathbf{H}_2^T & \dots & \mathbf{H}_K^T \end{bmatrix}^T$ as an aggregate channel matrix, the ZF constraint in (23) implies that

$$\mathbf{HW} = \begin{bmatrix} \sqrt{q_1} & & & \\ & \sqrt{q_2} & & \\ & & \ddots & \\ & & & \sqrt{q_K} \end{bmatrix} = \mathrm{diag}\{\sqrt{\mathbf{q}}\}, \quad (24)$$

where $\sqrt{\mathbf{q}} = \begin{bmatrix} \sqrt{q_1} & \sqrt{q_2} & \dots & \sqrt{q_K} \end{bmatrix}^T \in \mathbb{R}^{K \times 1}$ whose $i-$th element represents the channel gain of the $i-$th user. We thus can express $\mathbf{W}$ in the form

$$\mathbf{W} = \mathbf{H}^- \mathrm{diag}\{\sqrt{\mathbf{q}}\}, \qquad (25)$$

where $\mathbf{H}^-$ denotes the generalized inverse of $\mathbf{H}$, which can be any matrix that satisfies $\mathbf{HH}^-\mathbf{H} = \mathbf{H}$. Generally, the generalized inverse $\mathbf{H}^-$ is not unique. One of the special generalized inverse is the pseudo-inverse $\mathbf{H}^\dagger = \mathbf{H}^T(\mathbf{HH}^T)^{-1}$, which is known to have minimal Frobenius norm among all the generalized inverses. Different from RF systems where the pseudo-inverse is the optimum precoder under the total average power constraint [16], we show that for VLC systems, it is not necessary to be the optimal solution under amplitude constraint of VLC signals. Assuming that $\mathbf{H}$ is full row-rank, any generalized inverse $\mathbf{H}^-$ can be expressed by

$$\mathbf{H}^- = \mathbf{H}^\dagger + \mathbf{PQ}, \qquad (26)$$

where $\mathbf{P} = \mathbf{I} - \mathbf{H}^\dagger\mathbf{H}$ is the orthogonal projection onto the null space of $\mathbf{H}$ and, $\mathbf{Q}$ is an arbitrary matrix. Plugging (26) into (25), the general structure of any ZF precoding matrix $\mathbf{W}$ is given by

$$\mathbf{W} = \begin{bmatrix} \mathbf{H}^\dagger + \mathbf{PQ} \end{bmatrix} \mathrm{diag}\{\sqrt{\mathbf{q}}\}. \qquad (27)$$

This reduces the beamformer design problem for a certain performance metric to an optimization problem with respect to the $\mathbf{q}$ and the choice of generalized inverse $\mathbf{H}^-$ via $\mathbf{Q}$. In the next section, we investigate the optimal precoding designs for two typical performance measures in multiuser broadcast systems, namely: max-min fairness and maximum sum-rate.

V. OPTIMAL BEAMFORMER DESIGN

By removing the MUI via ZF precoders, the received signal at the $k-$th user simplifies to

$$y_k = \gamma \eta \mathbf{H}_k \mathbf{W}_k d_k + n_k. \qquad (28)$$

The goal of the precoding design is to find $\mathbf{W}_k$'s that maximize a performance measure under the amplitude signal constraint in (22) and the ZF constraint in (24), i.e.,

$$\begin{aligned} &\underset{\mathbf{q} \ge 0, \mathbf{W}}{\text{maximize}} \; f(\mathbf{q}) \\ &\text{subject to } \mathbf{HW} = \mathrm{diag}\{\sqrt{\mathbf{q}}\}, \\ &\qquad\qquad \left\|[\mathbf{W}]_{k,:}\right\|_1 \le \Delta_k \forall k, \end{aligned} \qquad (29)$$

where $f(\mathbf{q})$ is the objective function that represents the performance measure of interest. Denoting $\mathcal{C}_k$ as the rate of the $k-$user, typical performance measures include [39]

i) Sum rate: $f(\mathbf{q}) = \sum_{k=1}^{K} \mathcal{C}_k$.

ii) Proportional fairness: $f(\mathbf{q}) = \sum_{k=1}^{K} \log C_k$.

iii) Harmonic mean: $f(\mathbf{q}) = 1/\sum_{k=1}^{K} \frac{1}{C_k}$.

iv) Max-min fairness: $f(\mathbf{q}) = \min_{1 \leq k \leq K} C_k$,

with decreasing order of achievable sum rate and increasing order of user fairness.

Since the closed-form expression for C_k is not available, we rely on the lower and upper bounds of C_k developed in Section II. Noted that $d_k \in [-1, 1]$, the amplitude input signal is hence constrained within the range of $[-\gamma \eta \mathbf{H}_k \mathbf{W}_k, \gamma \eta \mathbf{H}_k \mathbf{W}_k]$. We therefore have the following lower and upper bounds for the rate of the k-th user

$$C_{L,k}^1 = \frac{1}{2} \log \left(1 + \frac{2\gamma \eta \mathbf{H}_k \mathbf{W}_k \mathbf{W}_k^T \mathbf{H}_k^T}{\pi e \sigma_k^2} \right), \quad (30)$$

$$C_{L,k}^2 = \log \left(\frac{2\gamma \eta \mathbf{H}_k \mathbf{W}_k}{\sqrt{2\pi e \sigma_k^2}} \right), \quad (31)$$

and

$$C_{U,k} = \sup_{\alpha_k \in [0,1]} \alpha_k \log \left(\frac{2\gamma \eta \mathbf{H}_k \mathbf{W}_k}{\sqrt{2\pi e \sigma_k^2}} \right) - \log \left(\alpha_k^{\alpha_k} (1 - \alpha_k)^{\frac{3}{2}(1-\alpha_k)} \right), \quad (32)$$

where $C_{L,k}^1$ and $C_{L,k}^2$ are two lower bounds derived from (3) and (4), respectively, while $C_{U,k}$ is the upper bound obtained from (5). Capitalizing on these bounds, we now investigate optimal precoding designs for two performance measures: the *max-min fairness* and the *maximum sum-rate*.

A. Max-Min Fairness

The max-min fairness criterion aims to maximize the minimum rate among users. It leads to the following optimization problem

$$\mathcal{P}1: \quad \underset{\mathbf{q} \geq \mathbf{0}, \mathbf{W}}{\text{maximize}} \ \min_k \ C_k$$
$$\text{subject to } \mathbf{HW} = \text{diag}\{\sqrt{\mathbf{q}}\},$$
$$\left\| [\mathbf{W}]_{k,:} \right\|_1 \leq \Delta_k \ \forall k.$$

1) Lower Bound: From the lower bound in (30), it is obvious that $C_{L,k}^1$ is proportional to q_k/σ_k^2. Let us define $\boldsymbol{\sigma} = \begin{bmatrix} \sigma_1^2 \ \sigma_2^2 \ \dots \ \sigma_K^2 \end{bmatrix}^T$ and $\text{diag}\{\mathbf{q}'\} = \text{diag}\{\mathbf{q}\}\text{diag}\{\boldsymbol{\sigma}\}^{-1}$ where $\mathbf{q}' = \begin{bmatrix} q_1' \ q_2' \ \dots \ q_K' \end{bmatrix}^T$. The optimization problem $\mathcal{P}1$ can thus be rewritten as

$$\mathcal{P}2: \quad \underset{\mathbf{q}' \geq \mathbf{0}, \mathbf{W}}{\text{maximize}} \ \min_k \ q_k'$$
$$\text{subject to } \mathbf{HW} = \text{diag}\{\sqrt{\mathbf{q}'}\}\text{diag}\{\sqrt{\boldsymbol{\sigma}}\},$$
$$\left\| [\mathbf{W}]_{k,:} \right\|_1 \leq \Delta_k \ \forall k.$$

Following the similar argument in [16], we can search the optimal solution of the form $\mathbf{q}' = q' \mathbf{1}$ for some q' is optimal. To see this, let $\mathbf{W}^*$ and $\mathbf{q}^*$ be the optimal solution to $\mathcal{P}2$ and we define new variables $\mathbf{q}' = \overline{q} \mathbf{1}$ and $\mathbf{W} = \mathbf{W}^* \text{diag}\left\{ \left[\sqrt{\overline{q}/q_1^*} \ \dots \ \sqrt{\overline{q}/q_K^*} \right] \right\}$, where $\overline{q} = \min_k q_k^*$. Then,

it holds that

$$\mathbf{HW} = \mathbf{HW}^* \text{diag}\left\{ \left[\sqrt{\overline{q}/q_1^*} \ \dots \ \sqrt{\overline{q}/q_K^*} \right] \right\}$$
$$= \text{diag}\{\sqrt{\mathbf{q}^*}\}\text{diag}\{\sqrt{\boldsymbol{\sigma}}\}\text{diag}\left\{ \left[\sqrt{\overline{q}/q_1^*} \ \dots \ \sqrt{\overline{q}/q_K^*} \right] \right\}$$
$$= \text{diag}\{\sqrt{\mathbf{q}'}\}\text{diag}\{\sqrt{\boldsymbol{\sigma}}\}, \quad (33)$$

and

$$\left\| [\mathbf{W}]_{k,:} \right\|_1 = \left\| \left[\mathbf{W}^* \text{diag}\left\{ \left[\sqrt{\overline{q}/q_1^*} \ \dots \ \sqrt{\overline{q}/q_K^*} \right] \right\} \right]_{k,:} \right\|_1$$
$$\leq \left\| [\mathbf{W}^*]_{k,:} \right\|_1, \quad (34)$$

since $\overline{q}/q_k^* \leq 1$ for all k. That is, $\mathbf{W}$ and $\mathbf{q}'$ are also feasible and offer the same objective. We thus can reduce $\mathcal{P}2$ to

$$\mathcal{P}3: \quad \underset{q' \geq 0, \mathbf{Q}}{\text{maximize}} \ q'$$
$$\text{subject to } \sqrt{q' \sigma_k^2} \left\| \left[\mathbf{H}^\dagger + \mathbf{PQ} \right]_{k,:} \right\|_1 \leq \Delta_k \ \forall k.$$

It is easy to see that the optimal solution q'_{opt} is given by

$$q'_{\text{opt}} = \frac{\Delta_k^2}{\max_k \sigma_k \left\| \left[\mathbf{H}^\dagger + \mathbf{PQ} \right]_{k,:} \right\|_1^2} \quad (35)$$

where $\mathbf{Q}$ is the solution to

$$\mathcal{P}4: \quad \underset{\mathbf{Q}, t}{\text{minimize}} \ t$$
$$\text{subject to } \sigma_k \left\| \left[\mathbf{H}^\dagger + \mathbf{PQ} \right]_{k,:} \right\|_1 \leq t \ \forall k.$$

The above problem is a linear programming, which has been extensively study [40] and can be solved efficiently by using standard optimization packages [42], [43].

2) Upper Bound: For the upper bound, the optimization problem is given by

$$\mathcal{P}5: \quad \underset{\alpha_k \in [0,1], \mathbf{q}' \geq \mathbf{0}, \mathbf{W}}{\text{maximize}} \ \min_k \ C_{U,k}$$
$$\text{subject to } \mathbf{HW} = \text{diag}\{\sqrt{\mathbf{q}'}\}\text{diag}\{\sqrt{\boldsymbol{\sigma}}\},$$
$$\left\| [\mathbf{W}]_{k,:} \right\|_1 \leq \Delta_k \ \forall k.$$

It is noted that $C_{U,k}$ is proportional to q_k' since the function $f(\alpha_k, q_k')_{\alpha_k \in [0,1]} = \alpha_k \log \left(\frac{2\gamma \eta \sqrt{q_k'}}{\sqrt{2\pi e}} \right) - \log \left(\alpha_k^{\alpha_k} (1 - \alpha_k)^{\frac{3}{2}(1-\alpha_k)} \right)$ is monotonically increase with respect to $\sqrt{q_k'}$ for a fixed α_k. Similar to the case of lower bound, we therefore can reduce problem $\mathcal{P}5$ to

$$\mathcal{P}6: \quad \underset{q' \geq 0, \mathbf{Q}}{\text{maximize}} \ q'$$
$$\text{subject to } \sqrt{q' \sigma_k^2} \left\| \left[\mathbf{H}^\dagger + \mathbf{PQ} \right]_{k,:} \right\|_1 \leq \Delta_k \ \forall k,$$

which gives the same solution as in (35). Given the optimal solution q'_{opt}, an upper bound for the fairness rate C_U of the users is given by

$$C_U = \sup_{\alpha_k \in [0,1]} \alpha_k \log \left(\frac{2\gamma \eta \sqrt{q'_{\text{opt}}}}{\sqrt{2\pi e}} \right) - \log \left(\alpha_k^{\alpha_k} (1 - \alpha_k)^{\frac{3}{2}(1-\alpha_k)} \right). \quad (36)$$

The solution for C_U can be obtained efficiently using the bisection method as described in Section II. B.

B. Maximum Sum-Rate

In multiuser systems, another typical performance metric is the maximum sum-rate of all users, which gives the following optimization problem

$$\mathcal{P}7: \; \underset{\mathbf{W}_k}{\text{maximize}} \; \sum_{k=1}^{K} C_k$$
$$\text{subject to } \mathbf{H}_i \mathbf{W}_k = 0 \;\; \forall k \neq i,$$
$$\sum_{i=1}^{K} \left\| [\mathbf{W}_i]_{k,:} \right\|_1 \leq \Delta_k \;\; \forall k.$$

1) Lower Bound: First, considering the lower bound in (30), the sum-rate maximization problem is written as

$$\mathcal{P}8: \; \underset{\mathbf{W}_k}{\text{maximize}} \; \frac{1}{2} \sum_{k=1}^{K} \log \left(1 + \frac{2\gamma \, \eta \mathbf{H}_k \mathbf{W}_k \mathbf{W}_k^T \mathbf{H}_k^T}{\pi e \sigma_k^2} \right)$$
$$\text{subject to } \mathbf{H}_i \mathbf{W}_k = 0 \;\; \forall k \neq i,$$
$$\sum_{i=1}^{K} \left\| [\mathbf{W}_i]_{k,:} \right\|_1 \leq \Delta_k \;\; \forall k.$$

It should be noted that the above problem is not a convex optimization problem with respect to $\mathbf{W}_k$ due to the non-convexity of the objective function. Thus, it is generally difficult (if not impossible) to optimally solve it in reasonable time. We therefore attempt to study a sub-optimal solution by finding a local optimality. To do that, let us introduce slack variables λ_k and express $\mathbf{H}_k \mathbf{W}_k = \sqrt{q_k}$. Problem $\mathcal{P}8$ is then rewritten as

$$\mathcal{P}9: \; \underset{\mathbf{W}_k, q_k, \lambda_k}{\text{maximize}} \; \frac{1}{2} \sum_{k=1}^{K} \log \left(1 + \frac{2\gamma \, \eta \lambda_k}{\pi e \sigma_k^2} \right)$$
$$\text{subject to } \mathbf{HW} = \text{diag}\left\{ \left[\sqrt{q_1} \; \cdots \; \sqrt{q_K} \right]^T \right\},$$
$$\sum_{i=1}^{K} \left\| [\mathbf{W}_i]_{k,:} \right\|_1 \leq \Delta_k \;\; \forall k,$$
$$q_k \geq \lambda_k \;\; \forall k,$$
$$q_k \geq 0 \;\; \forall k.$$

It can be seen that the objective function of the above problem is now concave. However, the first constraint is not convex since $\mathbf{HW}$ is affine but $\text{diag}\left\{ \left[\sqrt{q_1} \; \cdots \; \sqrt{q_K} \right]^T \right\}$ is concave.

To deal with this issue, we adopt the convex-concave procedure (CCCP) [44], [45], which involves an iterative process, to find a local optimal solution. Specifically, at the i-th iteration of the procedure, we approximately linearize the concave term $\sqrt{q_k}$ by using its Taylor expansion as $\sqrt{q_k} \approx \sqrt{q_k^{(i-1)}} + \frac{1}{2\sqrt{q_k^{(i-1)}}}\left(q_k - q_k^{(i-1)} \right)$, where $q_k^{(i-1)}$ is the value of q_k obtained from the previous iteration. As a result, problem $\mathcal{P}9$ can be transformed to a convex optimization problem as problem $\mathcal{P}10$ on the bottom of this page. The detailed iterative algorithm for solving $\mathcal{P}9$ is described in **Algorithm 1**.

Algorithm 1 Iterative Algorithm for Solving Problem $\mathcal{P}9$

1: **Initialization**
   1) Estimate channel matrices $\mathbf{H}_k$ and noise variances σ_k^2.
   2) Initialize q_k to be positive and sufficiently small, e.g., $q_k = 0.1$.

2: **Iteration**: At the $i-$th iteration
   1) Update $q_k^{(i)}$, λ_k, $\mathbf{W}_k$ given $q_k^{(i-1)}$ by solving problem $\mathcal{P}10$ using CVX toolbox .
   2) $i = i + 1$.

3: **Termination**: terminate the iteration when
   1) $|q_k^{(i)} - q_k^{(i-1)}| \leq \epsilon$, where $\epsilon = 10^{-3}$ is a predefined threshold, or
   2) $i = L$, where $L = 10$ is the predefined maximum number of iterations.

Due to the iterative nature, the Algorithm 1 usually requires several iterations to ensure a convergence of the solution. As a consequence, it may suffer from high computational time. We therefore present a simple lower bound solution for problem $\mathcal{P}8$ with lower complexity. For this purpose, we rely on the following observation

$$\frac{\left(\sum_{i=1}^{K} \left\| [\mathbf{W}_i]_{k,:} \right\|_1 \right)^2}{K} \leq \sum_{i=1}^{K} [\mathbf{W}_i \mathbf{W}_i^T]_{k,k} \;\; \forall k. \quad (37)$$

As proof, it is seen that $\left(\sum_{i=1}^{K} \left\| [\mathbf{W}_i]_{k,:} \right\|_1 \right)^2 = \left(\sum_{i=1}^{K} |w_{k,i}| \right)^2$ and $\sum_{i=1}^{K} \left[\mathbf{W}_i \mathbf{W}_i^T \right]_{k,k} = \sum_{i=1}^{K} w_{k,i}^2$. Hence,

---

$$\mathcal{P}10: \; \underset{\mathbf{W}_k, q_k^{(i)}, \lambda_k}{\text{maximize}} \; \frac{1}{2} \sum_{k=1}^{K} \log \left(1 + \frac{2\gamma \, \eta \lambda_k}{\pi e \sigma_k^2} \right)$$
$$\text{subject to } \mathbf{HW} = \text{diag}\left\{ \left[\sqrt{q_1^{(i-1)}} + \frac{1}{2\sqrt{q_1^{(i-1)}}}\left(q_1 - q_1^{(i-1)} \right) \; \cdots \; \sqrt{q_K^{(i-1)}} + \frac{1}{2\sqrt{q_K^{(i-1)}}}\left(q_K - q_K^{(i-1)} \right) \right]^T \right\},$$
$$\sum_{i=1}^{K} \left\| [\mathbf{W}_i]_{k,:} \right\|_1 \leq \Delta_k \;\; \forall k,$$
$$q_k^{(i)} \geq \lambda_k \;\; \forall k,$$
$$q_k^{(i)} \geq 0 \;\; \forall k.$$

the inequality in (37) can be obtained directly from the Cauchy-Schwarz inequality. By replacing the second constraint in $\mathcal{P}8$ by a stronger inequality as $\sum_{i=1}^{K} \left[\mathbf{W}_i \mathbf{W}_i^T \right]_{k,k} \leq \frac{\Delta_k^2}{K}$, we obtain the following optimization problem, which yields a lower bound solution to problem $\mathcal{P}8$

$$\mathcal{P}11: \; \underset{\mathbf{W}_k}{\text{maximize}} \; \frac{1}{2} \sum_{k=1}^{K} \log \left(1 + \frac{2\gamma\, \eta \mathbf{H}_k \mathbf{W}_k \mathbf{W}_k^T \mathbf{H}_k^T}{\pi e \sigma_k^2} \right)$$
$$\text{subject to} \quad \mathbf{H}_i \mathbf{W}_k = 0 \forall k \neq i,$$
$$\sum_{i=1}^{K} \left[\mathbf{W}_i \mathbf{W}_i^T \right]_{k,k} \leq \frac{\Delta_k^2}{K} \forall k.$$

Obviously, the tightness of this bound depends on the tightness of the inequality in (37), which is inversely proportional to the number of users. As illustrated in Section VI, a very tight lower bound solution to problem $\mathcal{P}8$ can be achieved when $K = 2$. For larger values, e.g., $K = 3$ and 4, acceptable lower bounds can still be obtained. Now, to solve problem $\mathcal{P}11$, let us define $\mathbf{G}_i = \mathbf{W}_i \mathbf{W}_i^T \succ 0$, resulting in

$$\mathcal{P}12: \; \underset{\mathbf{G}_k}{\text{maximize}} \; \frac{1}{2} \sum_{k=1}^{K} \log \left(1 + \frac{2\gamma\, \eta \mathbf{H}_k \mathbf{G}_k \mathbf{H}_k^T}{\pi e \sigma_k^2} \right)$$
$$\text{subject to} \quad \mathbf{H}_i \mathbf{G}_k \mathbf{H}_i^T = 0 \quad \forall k \neq i,$$
$$\sum_{i=1}^{K} \left[\mathbf{G}_i \right]_{k,k} \leq \frac{\Delta_k^2}{K} \quad \forall k,$$
$$\text{rank}(\mathbf{G}_k) = 1 \quad \forall k.$$

The objective function and the first two constraints of the above problem are convex with respect to $\mathbf{G}_k$. Unfortunately, the third constraint is not convex. To overcome this difficulty, we first omit that constraint to obtain

$$\mathcal{P}13: \; \underset{\mathbf{G}_k}{\text{maximize}} \; \frac{1}{2} \sum_{k=1}^{K} \log \left(1 + \frac{2\gamma\, \eta \mathbf{H}_k \mathbf{G}_k \mathbf{H}_k^T}{\pi e \sigma_k^2} \right)$$
$$\text{subject to} \quad \mathbf{H}_i \mathbf{G}_k \mathbf{H}_i^T = 0 \quad \forall k \neq i,$$
$$\sum_{i=1}^{K} \left[\mathbf{G}_i \right]_{k,k} \leq \frac{\Delta_k^2}{K} \quad \forall k.$$

It can be seen that problem $\mathcal{P}13$ is a standard determinant maximization (MAXDET) program subject to linear matrix inequalities [41], which can be solved efficiently by using standard optimization packages. An important question now is that whether the optimal solution of $\mathcal{P}13$ is also optimal to $\mathcal{P}11$. Interestingly in [16], it is proved that the rank-one constraint in $\mathcal{P}11$ always holds. In other words, problems $\mathcal{P}13$ and $\mathcal{P}11$ are equivalent and thus they have the same solution.

Now, we examine the use of the lower bound in (4), which accordingly leads to

$$\mathcal{P}14: \; \underset{\mathbf{W}_k}{\text{maximize}} \; \sum_{k=1}^{K} \log \left(\frac{2\gamma\, \eta \mathbf{H}_k \mathbf{W}_k}{\sqrt{2\pi e \sigma_k^2}} \right)$$
$$\text{subject to} \quad \mathbf{H}_i \mathbf{W}_k = 0 \quad \forall k \neq i,$$
$$\sum_{i=1}^{K} \left\| [\mathbf{W}_i]_{k,:} \right\|_1 \leq \Delta_k \quad \forall k.$$

The above optimization problem is also a MAXDET program subject to linear matrix inequalities. It therefore can be solved by using standard optimization packages.

2) Upper Bound: The sum-rate optimization problem with the use of the upper bound (32) can be written as

$$\mathcal{P}15: \; \underset{\alpha_k \in [0,1], \mathbf{W}_k}{\text{maximize}} \; \sum_{k=1}^{K} \alpha_k \log \left(\frac{2\gamma\, \eta \mathbf{H}_k \mathbf{W}_k}{\sqrt{2\pi e \sigma_k^2}} \right)$$
$$- \log \left(\alpha_k^{\alpha_k} (1 - \alpha_k)^{\frac{3}{2}(1-\alpha_k)} \right)$$
$$\text{subject to } \mathbf{H}_i \mathbf{W}_k = 0 \quad \forall k \neq i,$$
$$\sum_{i=1}^{K} \left\| [\mathbf{W}_i]_{k,:} \right\|_1 \leq \Delta_k \quad \forall k.$$

The objective function of problem $\mathcal{P}15$ is concave with respect to $\mathbf{W}_k$ and α_k. However, due to the special form of the objective function (containing a product of an affine and a concave function), most of standard optimization packages can not be used directly to solve $\mathcal{P}15$. To overcome this issue, we use an iterative approach. In particular, we iteratively optimize $\mathbf{W}_k$ and α_k while fixing the other variable. Fixing α_k, problem can be solved using CVX. On the other hand, when $\mathbf{W}_k$ are fixed, problem reduces to

$$\mathcal{P}16: \; \underset{\alpha_k \in [0,1]}{\text{maximize}} \; \sum_{k=1}^{K} f(\alpha_k),$$

where $f(\alpha_k) = \alpha_k \log \left(\frac{2\gamma\, \eta \mathbf{H}_k \mathbf{W}_k}{\sqrt{2\pi e \sigma_k^2}} \right) - \log \left(\alpha_k^{\alpha_k} (1 - \alpha_k)^{\frac{3}{2}(1-\alpha_k)} \right)$. Obviously, the optimal solution for problem $\mathcal{P}16$ is achieved when each summand $f(\alpha_k)$ of the objective function is maximized. Therefore, by solving optimal solutions for α_k using the bisection method, a solution for $\mathcal{P}15$ can easily be obtained. The proposed iterative algorithm is summarized in **Algorithm 2** as follows.

Algorithm 2 Iterative Algorithm for Optimizing $\mathbf{W}_k$ and α_k

1: **Initialization**
    1) Estimate channel matrices $\mathbf{H}_k$ and noise variances σ_k^2.
    2) Initialize precoding matrices $\mathbf{W}_k^{(0)}$, e.g., $\mathbf{W}_k^{(0)} = \mathbf{0}$.

2: **Iteration**: At the $i-$th iteration
    1) Update $\alpha_k^{(i)}$ given $\mathbf{W}_k^{(i-1)}$ by solving problem $\mathcal{P}16$ using the bisection method.
    2) With the obtained $\alpha_k^{(i)}$, solve problem $\mathcal{P}15$ to update $\mathbf{W}_k^{(i)}$ by using CVX toolbox.
    3) $i = i + 1$.

3: **Termination**: terminate the iteration when
    1) $\|\mathbf{W}_k^{(i)} - \mathbf{W}_k^{(i-1)}\|_F^2 \leq \epsilon$, where $\epsilon = 10^{-3}$ is a predefined threshold, or
    2) $i = L$, where $L = 10$ is the predefined maximum number of iterations.
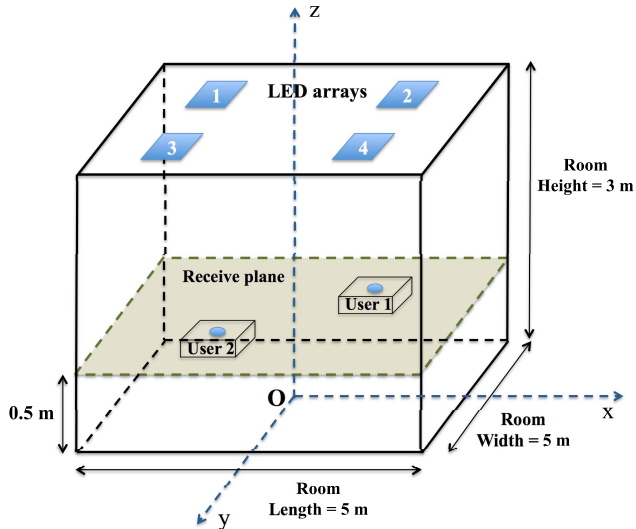

Fig. 4. Geometrical configuration of a MU-MISO VLC system with 4 LED arrays and 2 users.

VI. Numerical Results & Discussions

This section presents numerical results to illustrate the theoretical analyses of the max-min fairness and the maximum sum-rate performances. Figure 4 shows the geometrical configuration of the considered MU-MISO VLC system, which consists of 4 LED arrays. We assume that all receivers are placed on the same receive plane, which is 0.5 m above the floor. In addition, for the sake of convenience, a Cartesian coordinate system whose the origin is the center of the floor is used for specifying the positions of users and the LED arrays. Unless otherwise noted, the parameters of the room, LED arrays and optical receivers are given in Table I. Furthermore, all analytical results are obtained by averaging 10, 000 different channel realizations (10, 000 different positions of users are uniformly placed on the receive plane).

First, we compare the pseudo-inverse with the generalized inverse design in terms of the max-min fairness performance. The purpose is to validate our argument that, unlike its RF counterpart, the pseudo-inverse, which was studied in previous works [25], [26], may not necessarily result in the optimal solution in MU-MISO VLC system due to the amplitude constraint. In Fig. 5, we present the averaged normalized fairness power, which is defined as $\gamma\,\eta\sqrt{q'_{\text{opt}}}$, versus the number of LED arrays for different optimal designs of precoding matrix: the generalized inverse and the pseudo inverse. The number of users is set to $K = 2$ and the average transmitted power per LED array is set to 30 dBm. In addition, because the positions of LED arrays have an impact on the performance, for the sake of comparison, we assume that LED arrays are placed on a 2 meter radius circle so that the center points of them form a regular polygon as in Fig. 6 for the scenarios of $N_T = 2$, 3, 5 and 6 (the case of $N_T = 4$ was specified in Table I). It is seen that the generalized inverse precoding clearly outperforms the pseudo inverse, especially when the number of LED arrays is lager than the number of users. Particularly, the pseudo inverse becomes drastically inferior to the optimal design as the number of LED arrays increases.

TABLE I
MU-MISO VLC System Parameters

| Parameter	Value
Room and LED configurations	
Room Dimension (Length × Width × Height)	5 (m) × 5 (m) × 3 (m)
Number of LED arrays, N_T	4
LED array size	0.1 (m) × 0.1 (m)
Number of LED chips per array	36
LED array positions	array 1 : $(-\sqrt{2}, -\sqrt{2}, 3)$ array 2 : $(\sqrt{2}, -\sqrt{2}, 3)$ array 3 : $(-\sqrt{2}, \sqrt{2}, 3)$ array 4 : $(\sqrt{2}, \sqrt{2}, 3)$
LED bandwidth, B	20 MHz
LED beam angle, ϕ (LED Lambertian order is 1)	120°
LED conversion factor, η	0.44 W/A
Receiver photodetectors	
PD active area, A_r	1 cm^2
PD responsivity, γ	0.54 A/W
PD field of view (FOV), Ψ_c	60°
Optical filter gain, $T_s(\psi)$	1
Refractive index of the concentrator, κ	1.5
Other parameters	
Ambient light photocurrent, χ_{amb}	10.93 A/(m^2 · Sr)
Preamplifier noise current density, i_{amb}	5 pA/Hz$^{-1/2}$
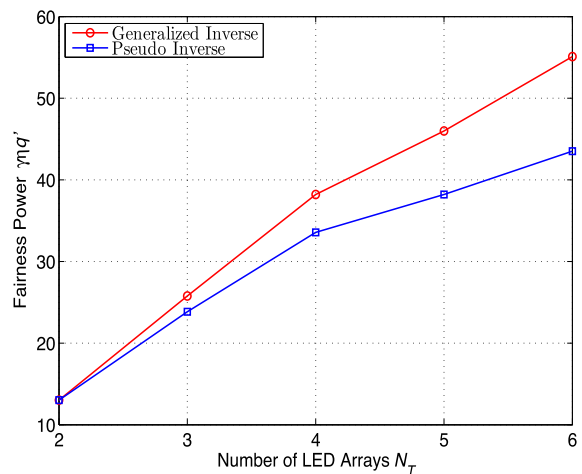
Fig. 5. Averaged normalized fairness power for different precoding matrix designs: generalized inverse and pseudo inverse.

This is because the pseudo inverse design restricts the search for the optimal solution into a much smaller feasible subset, i.e., restricting $\mathbf{Q} = \mathbf{0}$.

Next, Figs. 7, 8 and 9 present the averaged sum max-min fairness capacity versus the average LED array power P_s for 2-, 3-, and 4-user scenarios, respectively, with generalized and pseudo inverses. The average LED array power ranges from 20 to 40 dBm, which corresponds to 0.1 to 10 W. As expected from the previous figure, the generalized inverse performs better than the pseudo inverse does in all cases, especially
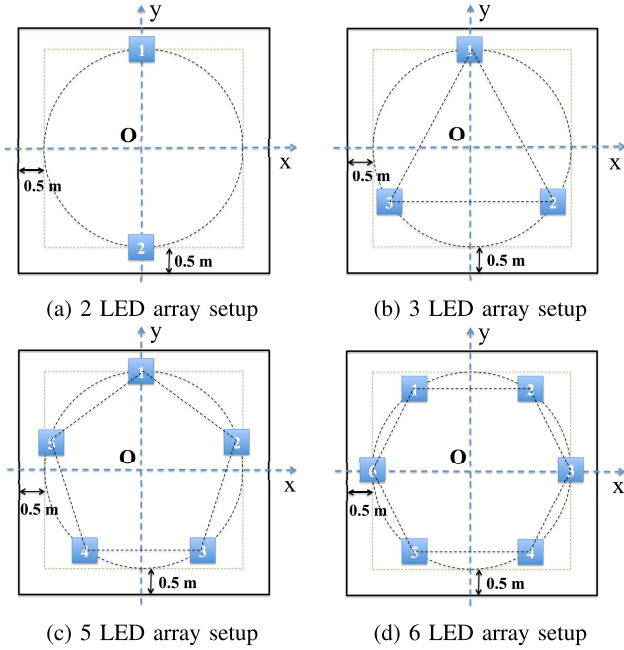
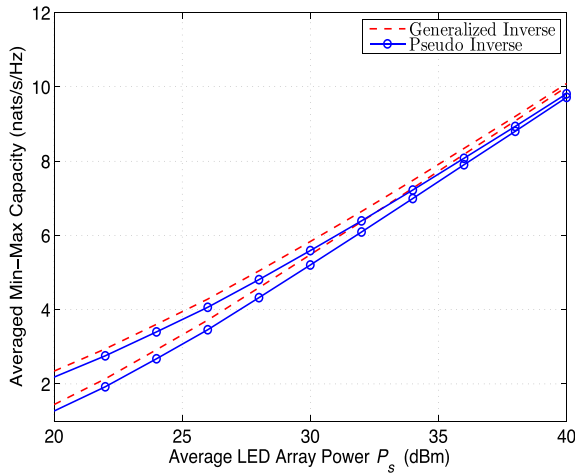Fig. 6. Examples of LED array setup.

(a) 2 LED array setup

(b) 3 LED array setup

(c) 5 LED array setup

(d) 6 LED array setup

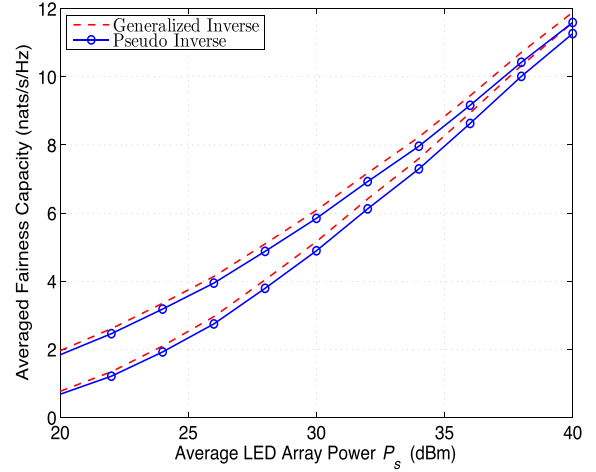Fig. 7. Averaged sum max-min fairness rate versus average LED array power: 2 users.

Fig. 8. Averaged sum max-min fairness rate versus average LED array power: 3 users.
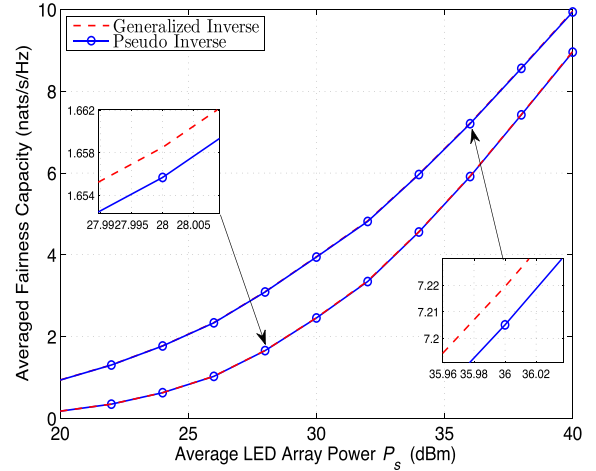

Fig. 9. Averaged sum max-min fairness rate versus average LED array power: 4 users.
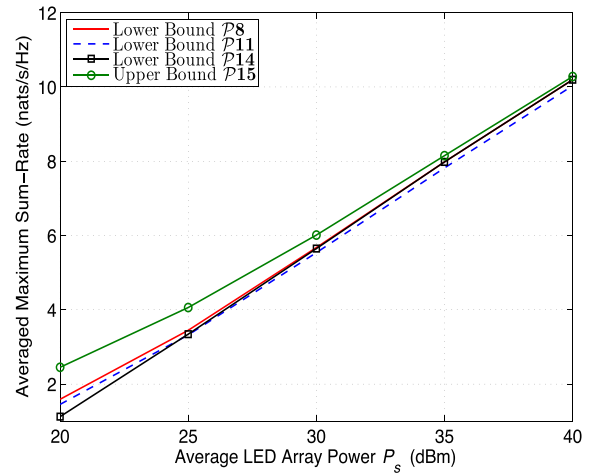

Fig. 10. Averaged sum-rate maximization versus average LED array power: 2 users.

in the high power regime. Nevertheless, it is seen that the superiority of the generalized inverse over the pseudo inverse decreases with an increase in the number of users. Especially, when the numbers of users and LED arrays are the same, i.e., $N_T = K = 4$ in Fig. 9 or when $N_T = 2 = K$ in Fig. 5, the performances of the generalized inverse precoding and the pseudo inverse precoding are almost identical.

We demonstrate in Figs. 10, 11 and 12 the averaged sum capacity versus the average LED array power for 2-, 3- and 4-user scenarios, respectively. Firstly, as expected from Proposition 1, all the bounds asymptotically converge at high transmitted power. It is observed that the rate of convergence is inversely proportional to the number of users, which is an obvious consequence of the sum-rate performance. Secondly, for the whole range of transmitted LED array power, the lower bound in $\mathcal{P}8$ is tight compared to the lower bound in $\mathcal{P}11$ with maximum gaps are 0.4 nat and 0.5 nat for 3 and 4 user scenarios, respectively, (the gap is negligible when there

are 2 users). On the other hand, the lower bound in $\mathcal{P}14$ is applicable in the high transmitted power only for the case of 3 and 4 users.

In Fig. 13a and Fig. 13b, the convergence behaviors of Algorithm 1 and Algorithm 2 for different numbers of users
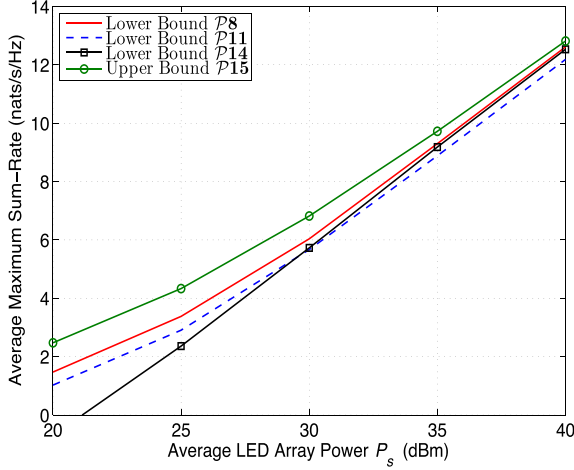
Fig. 11. Averaged sum-rate maximization versus average LED array power: 3 users.
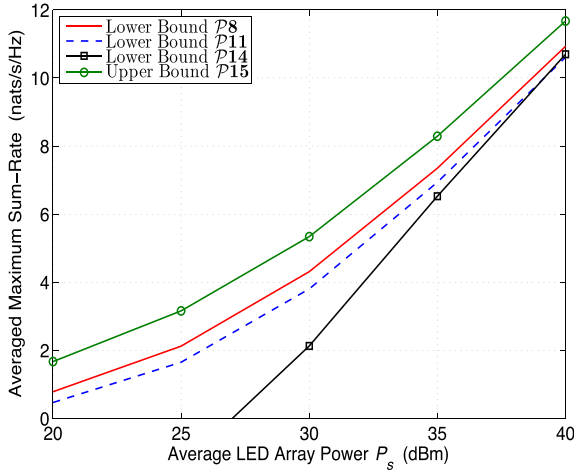

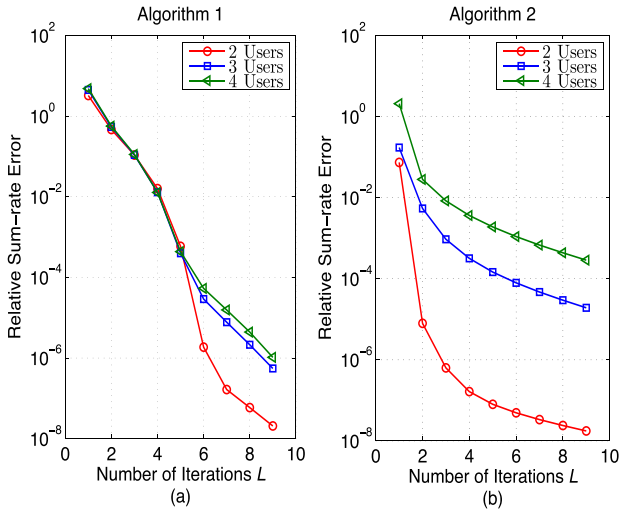Fig. 12. Averaged sum-rate maximization versus average LED array power: 4 users.

Fig. 13. (a) Convergence behavior of Algorithm 1, (b) Convergence behavior of Algorithm 2.

are presented, respectively. The average transmitted LED array power is set to 40 dBm. Specifically, at a targeted relative sum-rate error of $\epsilon_{\text{sum-rate}} = 10^{-3}$, the Algorithm 1 requires 5 iterations for all cases of the number of users. For the case

of the Algorithm 2, it needs 2, 3 and 6 iterations when the number of users are 2, 3 and 4, respectively, to obtain the relative sum-rate error of 10^{-3}.

VII. CONCLUSIONS

The paper studied optimal precoding designs for MU-MISO VLC systems with practical constraints of the optical signal. To mitigate the MUI among users, ZF precoding technique is utilized due to its computational advantage. Unlike previous studies, optimal ZF precoding matrices are designed in accordance with specific performance criterions. Capitalizing on the precoding designs, lower and upper bounds of the max-min fairness and the maximum sum-rate are derived. Numerical results showed that the generalized inverse design achieves better performance than that of the pseudo inverse design, especially in the high SNR region.

APPENDIX
PROOF OF PROPOSITION 1

The first derivative of $f(\alpha)$ is given by

$$f'(\alpha) = \log\left(\frac{2A}{\sqrt{2\pi e N_0}}\right) - \log(\alpha) + \frac{3}{2}\log(1-\alpha) + \frac{1}{2}. \tag{38}$$

Since $f'(\alpha)$ is continuous, monotonically decreasing over $(0, 1)$, $\lim_{\alpha \to 0} f'(\alpha) = \infty$ and $\lim_{\alpha \to 1} f'(\alpha) = -\infty$, the critical point α^* exists and is unique. At the critical point

$$f_1(\alpha^*) = \log(\alpha^*) - \frac{3}{2}\log(1-\alpha^*) = \log\left(\frac{2A}{\sqrt{2\pi e N_0}}\right) + \frac{1}{2}. \tag{39}$$

As

$$\lim_{\frac{A}{\sqrt{N_0}} \to 0} \log\left(\frac{2A}{\sqrt{2\pi e N_0}}\right) + \frac{1}{2} = -\infty, \tag{40}$$

$$\lim_{\frac{A}{\sqrt{N_0}} \to \infty} \log\left(\frac{2A}{\sqrt{2\pi e N_0}}\right) + \frac{1}{2} = \infty, \tag{41}$$

$$\lim_{\alpha^* \to 0} f_1(\alpha^*) = -\infty, \tag{42}$$

$$\lim_{\alpha^* \to 1} f_1(\alpha^*) = \infty \tag{43}$$

and $f_1(\alpha^*)$ is continuous, monotonically increasing, we deduce to

$$\lim_{\frac{A}{\sqrt{N_0}} \to 0} \alpha^* = 0 \text{ and } \lim_{\frac{A}{\sqrt{N_0}} \to \infty} \alpha^* = 1. \tag{44}$$

As a result

$$\lim_{\frac{A}{\sqrt{N_0}} \to 0} C_U = f(0) = 0, \tag{45}$$

$$\lim_{\frac{A}{\sqrt{N_0}} \to \infty} C_U = f(1) = \log\left(\frac{2A}{\sqrt{2\pi e N_0}}\right). \tag{46}$$

This completes the proof.

REFERENCES

[1] A. Nuwanpriya, S.-W. Ho, and C. S. Chen, "Indoor MIMO visible light communications: Novel angle diversity receivers for mobile users," *IEEE J. Sel. Areas Commun.*, vol. 33, no. 9, pp. 1780–1792, Sep. 2015.

[2] P. H. Pathak, X. Feng, P. Hu, and P. Mohapatra, "Visible light communication, networking, and sensing: A survey, potential and challenges," *IEEE Commun. Surveys Tuts.*, vol. 17, no. 4, pp. 2047–2077, 4th Quart., 2015.

[3] A. Jovicic, J. Li, and T. Richardson, "Visible light communication: Opportunities, challenges and the path to market," *IEEE Commun. Mag.*, vol. 51, no. 12, pp. 26–32, Dec. 2013.

[4] A. C. Boucouvalas, P. Chatzimisios, Z. Ghassemlooy, M. Uysal, and K. Yiannopoulos, "Standards for indoor optical wireless communications," *IEEE Commun. Mag.*, vol. 53, no. 3, pp. 24–31, Mar. 2015.

[5] *IEEE Standard for Local and Metropolitan Area Networks—Part 15.7: Short-Range Wireless Optical Communication Using Visible Light*, IEEE Standard 802.15.7, Mar. 2011.

[6] P. A. Haigh, Z. Ghassemlooy, S. Rajbhandari, I. Papakonstantinou, and W. Popoola, "Visible light communications: 170 Mb/s using an artificial neural network equalizer in a low bandwidth white light configuration," *J. Lightw. Technol.*, vol. 32, no. 9, pp. 1807–1813, May 1, 2014.

[7] D. A. Basnayaka and H. Haas, "Hybrid RF and VLC systems: Improving user data rate performance of VLC systems," in *Proc. IEEE Veh. Technol. Conf. (VTC-Spring)*, May 2015, pp. 1–5.

[8] J.-H. Yoo and S.-Y. Jung, "Multi-coded variable PPM with level cutting for high data rate visible light communications," in *Proc. Asia–Pacific Conf. Commun. (APCC)*, Oct. 2012, pp. 703–708.

[9] L. Zeng *et al.*, "High data rate multiple input multiple output (MIMO) optical wireless communications using white LED lighting," *IEEE J. Sel. Areas Commun.*, vol. 27, no. 9, pp. 1654–1662, Dec. 2009.

[10] T. Fath and H. Haas, "Performance comparison of MIMO techniques for optical wireless communications in indoor environments," *IEEE Trans. Commun.*, vol. 61, no. 2, pp. 733–742, Feb. 2013.

[11] L. Wu, Z. Zhang, and H. Liu, "MIMO-OFDM visible light communications system with low complexity," in *Proc. IEEE Int. Conf. Commun. (ICC)*, Jun. 2013, pp. 3933–3937.

[12] A. Burton, H. L. Minh, Z. Ghassemlooy, E. Bentley, and C. Botella, "Experimental demonstration of 50-Mb/s visible light communications using 4 × 4 MIMO," *IEEE Photon. Technol. Lett.*, vol. 26, no. 9, pp. 945–948, May 1, 2014.

[13] A. H. Azhar, T. Tran, and D. O'Brien, "A gigabit/s indoor wireless transmission using MIMO-OFDM visible-light communications," *IEEE Photon. Technol. Lett.*, vol. 52, no. 2, pp. 171–174, Jan. 15, 2013.

[14] K. Ying, H. Qian, R. J. Baxley, and G. T. Zhou, "MIMO transceiver design in dynamic-range-limited VLC systems," *IEEE Photon. Technol. Lett.*, vol. 28, no. 22, pp. 2593–2596, Nov. 15, 2016.

[15] K. Ying, H. Qian, R. J. Baxley, and S. Yao, "Joint optimization of precoder and equalizer in MIMO VLC systems," *IEEE J. Sel. Areas Commun.*, vol. 33, no. 9, pp. 1948–1958, Sep. 2015.

[16] A. Wiesel, Y. C. Eldar, and S. Shamai, "Zero-forcing precoding and generalized inverses," *IEEE Trans. Signal Process.*, vol. 56, no. 9, pp. 4409–4418, Sep. 2008.

[17] Q. H. Spencer, A. L. Swindlehurst, and M. Haardt, "Zero-forcing methods for downlink spatial multiplexing in multiuser MIMO channels," *IEEE Trans. Signal Process.*, vol. 52, no. 2, pp. 461–471, Feb. 2004.

[18] C. B. Peel, B. M. Hochwald, and A. L. Swindlehurst, "A vector-perturbation technique for near-capacity multiantenna multiuser communication—Part I: Channel inversion and regularization," *IEEE Trans. Commun.*, vol. 53, no. 1, pp. 195–202, Jan. 2005.

[19] V. Stankovic and M. Haardt, "Generalized design of multi-user MIMO precoding matrices," *IEEE Trans. Wireless Commun.*, vol. 7, no. 3, pp. 953–961, Mar. 2008.

[20] H. Yang, J. Chen, Z. Wang, and C. Yu, "Performance of a precoding MIMO system for decentralized multiuser indoor visible light communications," *IEEE Photon. J.*, vol. 5, no. 4, Aug. 2013, Art. no. 7800211.

[21] J. Chen, N. Y. Ma; Hong, and C. Yu, "On the performance of MU-MIMO indoor visible light communication system based on THP algorithm," in *Proc. IEEE/CIC Int. Conf. Commun. China*, Oct. 2014, pp. 136–140.

[22] T. V. Pham, H. L. Minh, Z. Ghassemlooy, T. Hayashi, and A. T. Pham, "Sum-rate maximization of multi-user MIMO visible light communications," in *Proc. IEEE Int. Conf. Commun. Workshop (ICCW)*, Jun. 2015, pp. 1344–1349.

[23] H. Ma, L. Lampe, and S. Hranilovic, "Coordinated broadcasting for multiuser indoor visible light communication systems," *IEEE Trans. Commun.*, vol. 63, no. 9, pp. 3313–3324, Sep. 2015.

[24] B. Li, J. Wang, R. Zhang, H. Shen, C. Zhao, and L. Hanzo, "Multiuser MISO transceiver design for indoor downlink visible light communication under per-LED optical power constraints," *IEEE Photon. J.*, vol. 7, no. 4, Aug. 2015, Art. no. 7201415.

[25] Z. Yu, R. J. Baxley, and G. T. Zhou, "Multi-user MISO broadcasting for indoor visible light communication," in *Proc. IEEE Int. Conf. Acoust., Speech Signal Process. (ICASSP)*, May 2013, pp. 4849–4853.

[26] T. Cogalan, H. Haas, and E. Panayirci, "Precoded single-cell multi-user MISO visible light communications," in *Proc. 21th Eur. Wireless Conf.*, May 2015, pp. 1–6.

[27] T. V. Pham and A. T. Pham, "Max-min fairness and sum-rate maximization of MU-VLC local networks," in *Proc. IEEE Globecom Workshops (GC Wkshps)*, pp. 1–6, Dec. 2015.

[28] T. V. Pham and A. T. Pham, "On the secrecy sum-rate of MU-VLC broadcast systems with confidential messages," in *Proc. Int. Symp. Commun. Syst., Net. Digit. Signal Process. (CSNDSP)*, Jul. 2016, pp. 1–6.

[29] K.-H. Park, Y.-C. Ko, and M.-S. Alouini, "On the power and offset allocation for rate adaptation of spatial multiplexing in optical wireless MIMO channels," *IEEE Trans. Commun.*, vol. 61, no. 4, pp. 1535–1543, Apr. 2013.

[30] J. G. Smith, "The information capacity of amplitude- and variance-constrained sclar Gaussian channels," *Inf. Control*, vol. 18, no. 3, pp. 203–219, Apr. 1971.

[31] A. Lapidoth, S. M. Moser, and M. A. Wigger, "On the capacity of free-space optical intensity channels," *IEEE Trans. Inf. Theory*, vol. 55, no. 10, pp. 4449–4461, Oct. 2009.

[32] A. A. Farid and S. Hranilovic, "Capacity bounds for wireless optical intensity channels with Gaussian noise," *IEEE Trans. Inf. Theory*, vol. 56, no. 12, pp. 6066–6077, Dec. 2010.

[33] C. E. Shannon, "A mathematical theory of communication," *Bell Syst. Tech. J.*, vol. 27, no. 3, pp. 379–423, 1948.

[34] T. Cover and J. Thomas, *Elements of Information Theory*. Hoboken, NJ, USA: Wiley, 2006.

[35] A. Chaaban, J.-M. Morvan, and M.-S. Alouini, "Free-space optical communications: Capacity bounds, approximations, and a new sphere-packing perspective," *IEEE Trans. Commun.*, vol. 64, no. 3, pp. 1176–1191, Mar. 2016.

[36] T. Young and M. J. Mohlenkamp, *Introduction to Numerical Methods and MATLAB Programming for Engineers*, Dept. Math. Athens, OH, USA: Ohio Univ., 2015.

[37] Y. Tanaka, T. Komine, S. Haruyama, and M. Nakagawa, "Indoor visible light data transmission system utilizing white LED lights," *IEICE Trans. Commun.*, vol. E86-B, no. 8, pp. 2440–2454, 2003.

[38] T. Komine and M. Nakagawa, "Fundamental analysis for visible-light communication system using LED lights," *IEEE Trans. Consum. Electron.*, vol. 50, no. 1, pp. 100–107, Feb. 2004.

[39] Z.-Q. Luo and S. Zhang, "Dynamic spectrum management: Complexity and duality," *IEEE J. Sel. Topics Signal Process.*, vol. 2, no. 1, pp. 57–73, Feb. 2008.

[40] S. Boyd and L. Vandenberghe, *Convex Optimization*. Cambridge, U.K.: Cambridge Univ. Press, 2004.

[41] L. Vandenberghe, S. Boyd, and S. P. Wu, "Determinant maximization with linear matrix inequality constraints," *SIAM J. Matrix Anal. Appl.*, vol. 19, no. 2, pp. 499–533, Apr. 1998.

[42] M. Grant and S. Boyd. (Jan. 2015). *CVX: Matlab Software for Disciplined Convex Programming Version 2.1*. [Online]. Available: http://cvxr.com/cvx/

[43] J. Löfberg, "YALMIP : A toolbox for modeling and optimization in MATLAB," in *Proc. IEEE Int. Symp. Comput. Aided Control Syst. Design*, Sep. 2004, pp. 284–289.

[44] A. L. Yuille and A. Rangarajan, "The concave-convex procedure (CCCP)," *Neural Comput.*, vol. 15, no. 4, pp. 915–936, Apr. 2003.

[45] B. K. Sriperumbudur and G. R. G. Lanckriet, "On the convergence of the concave-convex procedure," in *Proc. Neural Inf. Process. Syst.*, 2009, pp. 1759–1767.

Thanh V. Pham (S'13) received the B.E. and M.E. degrees in computer network systems from The University of Aizu, Japan, in 2014 and 2016, respectively, where he is currently pursuing the Ph.D. degree. His study in Japan was funded by the Japanese Government Scholarship (MonbuKagakusho). His research interests are in the area of free space optics, relay networks, and visible light communications. He is a Student Member of the IEICE.

Hoa Le-Minh was a Researcher with Siemens AG, Munich, Germany, in 2002, and the University of Oxford, U.K., in 2010. Since 2010, he has been with Northumbria University, U.K., where he served as a Senior Lecturer in 2010 and then a Program Leader of Electrical and Electronics Engineering in 2013. He has authored over 100 papers published in referred journals and conferences. His research interests include optical communications, visible-light communications, and smartphone technology. He currently serves as the Vice-Chair of the IEEE Communications Chapter of U.K. and Ireland, and also serves as a Guest Editor of the IET and ETT journals.

Anh T. Pham (SM'00) received the B.E. and M.E. degrees in electronics engineering from the Hanoi University of Technology, Vietnam, in 1997 and 2000, respectively, and the Ph.D. degree in information and mathematical sciences from Saitama University, Japan, in 2005. From 1998 to 2002, he was with NTT Corporation, Vietnam. Since 2005, he has been a Faculty Member with The University of Aizu, where he is currently a Professor and the Head of the Computer Communications Laboratory, Division of Computer Engineering. His research interests are in the broad areas of communication theory and networking with a particular emphasis on modeling, design, and performance evaluation of wired/wireless communication systems and networks. He has authored/co-authored over 150 peer-reviewed papers on these topics. He is a member of the IEICE and the OSA.